[5] W. Getsinger, "Microstrip dispersion model," *IEEE Trans. Microwave Theory Tech.*, vol. MTT-21, pp. 34–39, Jan. 1973.
[6] M. Culton, "Film technology in microwave integrated circuits," *IEEE Trans. Microwave Theory Tech.*, vol. MTT-19, pp. 1481–1489, Oct. 1971.
[7] W. D. Hutchins, "Microwave design utilization with a new nonceramic high-dielectric substrate," IBM-Federal Syst. Division Publ., Owego, N.Y. 13827, IBP Rep. 77, TPA 0026, 1977.
[8] E. H. England, "A coaxial to microstrip transition," *IEEE Trans. Microwave Theory Tech.*, vol. MTT-24, pp. 47–48, Jan. 1976.

A Variational Theory for Wave Propagation in Inhomogeneous Dielectric Slab Loaded Waveguides

CHANG-TSUO LIU AND CHUN HSIUNG CHEN

Abstract—**A novel numerical technique based on the variational formulation defined only in the slab is developed to study the loaded rectangular waveguide with an inhomogeneous dielectric slab. The variational equation for the boundary value problem is formulated and solved numerically, using the finite element method with piecewise quadratic trial functions. A comparison of this new technique with the conventional variational ones is presented. Various propagation characteristics, such as the phase constant, useful bandwidth, power handling capacity, and attenuation constants due to conductor and dielectric losses, are investigated for the waveguide centrally loaded with a slab of parabolic dielectric profile. The effects of changes in dielectric profiles are discussed by examining the results for the slabs with constant and parabolic profiles.**

I. Introduction

RECTANGULAR waveguides loaded with dielectric slabs have been investigated extensively by many authors [1]–[14], and found possessing applications such as differential phase shifter, filter, and harmonic frequency separator. Most previous investigations were limited to the problems for which the loaded slabs (symmetrical or asymmetrical) are homogeneous. Thus the efficient field-matching technique [14] can be applied and the characteristic equations for cutoff frequencies and propagation constants can readily be obtained and solved graphically or numerically. For the waveguides loaded with arbitrary inhomogeneous dielectrics, the approach of finding the solutions analytically [9], [10], [15] is in general impractical, and, therefore, other techniques such as the variational (Ritz) method [2], [8], [14] have to be considered instead. Although the Ritz method is useful in solving the problem with symmetrically loaded slabs, it is awkward in handling the asymmetrically loaded one with discontinuous permittivities. The purpose of this study is to establish a new variational formulation which is defined only in the slab so that it can effectively circumvent the aforementioned difficulty due to the permittivity discontinuities. Another purpose is to provide various propagation characteristics, for the rectangular waveguide loaded with a slab of parabolic profile, which are not available in the literature.

Manuscript received October 6, 1980; revised February 24, 1981. This work was supported by the National Science Council, Republic of China, under Grant NSC-69E-0201-02(20).

The authors are with the Department of Electrical Engineering, National Taiwan University, Taipei, Taiwan, Republic of China.

II. Formulations

Let us consider the uniform rectangular metallic tube of width a and height b ($a \geq b$) loaded with an inhomogeneous dielectric slab of $(\mu_0, \epsilon_0\epsilon_r(x))$ from $x=c$ to $x=c+d$ as shown in Fig. 1. The conductor and dielectric losses are assumed to be small and will be neglected at the beginning of this study.

For this configuration it is convenient to use LSE and LSM modes to describe the wave fields [2]. Mathematically, the fields (with time factor $e^{j\omega t}$) of LSE (or LSM) modes can be derived from the magnetic- (or electric-) type Hertz vector potential $\overline{\Pi}_h$ (or $\overline{\Pi}_e$):

$$\overline{\Pi}_h(x, y, z) = \hat{x}\phi_h(x)\cos\left(\frac{n\pi y}{b}\right)e^{-jk_z z}, \qquad n=0,1,2,\cdots \tag{1a}$$

$$\overline{\Pi}_e(x, y, z) = \hat{x}\phi_e(x)\sin\left(\frac{n\pi y}{b}\right)e^{-jk_z z}, \qquad n=1,2,\cdots \tag{1b}$$

0018-9480/81/0800-0805$00.75 ©1981 IEEE

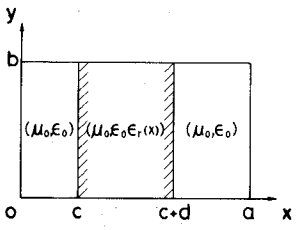

Fig. 1. Geometry of inhomogeneous dielectric slab loaded waveguide.

TABLE I
DEFINITIONS OF SYMBOLS IN (2) AND (7)

Symbol	LSE mode	LSM mode
$\phi(x)$	$\phi_h(x)$	$\phi_e(x)$
$p(x)$	1	$\begin{cases} 1, & 0\leq x<c,\quad c+d<x\leq a \\ \frac{1}{\epsilon_r(x)}, & c\leq x\leq c+d \end{cases}$
$r(x)$	$\begin{cases} 1, & 0\leq x<c,\quad c+d<x\leq a \\ \epsilon_r(x), & c\leq x\leq c+d \end{cases}$	1
a_{11}	0	1
a_{21}	0	1
a_{12}	1	0
a_{22}	1	0

where ϕ_h (or ϕ_e) satisfies the eigenvalue problem

$$-\frac{d}{dx}\left[p(x)\frac{d\phi(x)}{dx}\right]+\left[\left(\frac{n\pi}{b}\right)^2+k_z^2\right]p(x)\phi(x)=\xi r(x)\phi(x),\qquad 0<x<a$$

$$a_{11}\frac{d\phi}{dx}(0)+a_{12}\phi(0)=0$$

$$a_{21}\frac{d\phi}{dx}(a)+a_{22}\phi(a)=0. \tag{2}$$

The number ξ is interpreted as an eigenvalue

$$\xi=k^2=\omega^2\mu_0\epsilon_0 \tag{3}$$

and k_z is the propagation constant along the guide

$$k_z=\beta-j\alpha \tag{4}$$

where β and α are the phase and attenuation constants, respectively. The other symbols are given in Table I.

Of course, the wave field $\phi(x)$ should satisfy the continuity conditions for tangential E and H at the point $x_d(0<x_d<a)$ where the permittivity is discontinuous, i.e.,

$$\phi(x_d^-)=\phi(x_d^+) \tag{5a}$$

$$p(x_d^-)\frac{d\phi}{dx}(x_d^-)=p(x_d^+)\frac{d\phi}{dx}(x_d^+). \tag{5b}$$

The particular wave fields associated with (1a) and (1b) will be named the LSE_{mn} and LSM_{mn} modes, respectively, where the index m $(=1,2,\cdots)$ denotes the order of eigenvalues ξ_{mn} defined by (2), (3) and the one n describes the field variations in the y-direction as specified by (1). Physically, the particular eigenvalues $\xi_{c_{mn}}$ which correspond to $k_z=0$ may be identified with the cutoff frequencies $f_{c_{mn}}$ of the waveguide

$$\xi_{c_{mn}}=(2\pi f_{c_{mn}})^2\mu_0\epsilon_0. \tag{6}$$

The conventional variational equivalent of (2) can be written as

$$\delta I(\phi)=0$$

$$I(\phi)=\int_0^a\left\{p(x)\left(\frac{d\phi}{dx}\right)^2+\left[\left(\left(\frac{n\pi}{b}\right)^2+k_z^2\right)p(x)-\xi r(x)\right]\phi^2(x)\right\}dx \tag{7}$$

where $\phi(0)=\phi(a)=0$ for LSE modes, and $(d\phi)/(dx)(0)=(d\phi)/(dx)(a)=0$ or $\phi(0)$, $\phi(a)$ are unconstrained for LSM modes. For the case there exists permittivity discontinuity at x_d, the actual computation of the integral $\int_0^a$ in (7) should be separated into parts, $\int_0^{x_d^-}+\int_{x_d^+}^a$. In this manner, the continuity conditions (5) may be identified with the natural transition conditions of the variational formulation (7).

Conventionally, either Ritz or finite element method may be used for solving (7); the former may be better for the symmetrically loaded problem while the latter for the asymmetrically loaded one, as explained later.

The Ritz method usually chooses the harmonic trial function $\tilde{\phi}(x)$ such that

$$\tilde{\phi}(x)=\sum_i C_i u_i(x) \tag{8}$$

where

$$u_i(x)=\begin{cases}\sin\left(\dfrac{i\pi x}{a}\right), & i=1,2,\cdots, \quad \text{for LSE modes}\\ \cos\left(\dfrac{i\pi x}{a}\right), & i=0,1,2,\cdots, \quad \text{for LSM modes.}\end{cases} \tag{9}$$

Since the trial function (8) for LSM modes may violate the natural transition condition (5b) whenever there is a jump in permittivity at the air–slab interfaces, its use then makes the approximate solution very poorly convergent to the true one, especially when the jump is large. This difficulty has been circumvented, at least for the centrally loaded problem, by using the so-called hybrid trial functions as follows [14]:

$$u_i(x)=\cos\left(\frac{i\pi x}{a}\right), \quad 0\leqslant x\leqslant a, \quad i=0,2,\cdots. \tag{10}$$

$$u_i(x)=\begin{cases}\sin\left[\dfrac{i\pi(x-c)}{d}\right], & c\leqslant x\leqslant c+d\\ 0, & 0\leqslant x<c, \quad c+d<x\leqslant a\end{cases}, \quad i=1,3,\cdots.$$

However, this modification is still not efficient for the asymmetrically loaded problem [8].

The finite element method [16], which adopts piecewise polynomials as trial functions, may be useful in solving the variational problem (7) with an inhomogeneous slab loading. An advantage of this method is that the transition condition (5b) may be met naturally if the node points of the subdivision happen to coincide with the points of the profile discontinuities. Thus the aforementioned difficulty of using Ritz method for LSM modes can be avoided if finite element method is employed instead. In this study, the piecewise quadratic function

$$\begin{aligned}\tilde{\phi}(x)=&\phi_{i-1}\frac{(x-x_i)(x-x_{i+1})}{(x_{i-1}-x_i)(x_{i-1}-x_{i+1})}\\ &+\phi_i\frac{(x-x_{i-1})(x-x_{i+1})}{(x_i-x_{i-1})(x_i-x_{i+1})}\\ &+\phi_{i+1}\frac{(x-x_{i-1})(x-x_i)}{(x_{i+1}-x_{i-1})(x_{i+1}-x_i)},\\ &x\in[x_{i-1},x_{i+1}]\end{aligned} \tag{11}$$

will be chosen as the trial function for approximating the desired solution $\phi(x)$ in the element $[x_{i-1}, x_{i+1}]$, where $\phi_i=\tilde{\phi}(x_i)$ and x_i is a node of the subdivision. The points $x=c$ and $x=c+d$ should be chosen as the subdivision nodes, as explained before.

The approximate (or discrete) system corresponding to the variational problem (7), using Ritz method (8)–(10) or finite element method (11), can be written as

$$A\Phi=\xi B\Phi \tag{12}$$

where A and B are known square matrices, while Φ and ξ are eigenvector and eigenvalue to be determined. The column vector Φ is related to C_i or ϕ_i depending on whether Ritz or finite element method is employed.

The conventional variational formulation (7) is defined over the whole region $[0, a]$. Hence attention must be paid to the choice of the trial function for speeding convergence (Ritz method), or unnecessary subdivision must be made in the air regions where the field behavior is actually known (finite element method). This disadvantage can be avoided by taking advantage of the known solution behavior in the air regions and then formulating the variational equation only within the inhomogeneous slab [17].

Let us express the solution ϕ of (2) as

$$\phi_h(x)=\begin{cases}D_h\sinh(vx), & 0\leqslant x\leqslant c\\ \psi_h(x), & c\leqslant x\leqslant c+d\\ F_h\sinh[v(a-x)], & c+d\leqslant x\leqslant a\end{cases} \tag{13a}$$

for LSE modes, and

$$\phi_e(x)=\begin{cases}D_e\cosh(vx), & 0\leqslant x\leqslant c\\ \psi_e(x), & c\leqslant x\leqslant c+d\\ F_e\cosh[v(a-x)], & c+d\leqslant x\leqslant a\end{cases} \tag{13b}$$

for LSM modes where

$$v^2=k_z^2-k^2+\left(\frac{n\pi}{b}\right)^2 \tag{14}$$

$$n=\begin{cases}0,1,2,\cdots, & \text{for LSE modes}\\ 1,2,\cdots, & \text{for LSM modes}\end{cases}.$$

By matching the continuity conditions for tangential E and H at $x=c$ and $x=c+d$, one can obtain the alternative eigenvalue problem for $\psi_h(x)$ (or $\psi_e(x)$) as follows:

$$-\frac{d}{dx}\left[p(x)\frac{d\psi(x)}{dx}\right]+v^2p(x)\psi(x)=\xi[r(x)-p(x)]\psi(x), \quad c<x<c+d \tag{15a}$$

$$b_{11}\frac{d\psi}{dx}(c)+b_{12}\psi(c)=0 \tag{15b}$$

$$b_{21}\frac{d\psi}{dx}(c+d)+b_{22}\psi(c+d)=0 \tag{15c}$$

where ξ is defined by (3); v^2 by (14); $p(x)$, $r(x)$ are defined by Table I; and other symbols by Table II.

The new variational formulation, which is defined in the slab and also equivalent to (15), is as follows:

$$\delta I(\psi)=0 \tag{16}$$

$$\begin{aligned}I(\psi)=&\int_c^{c+d}\left\{p(x)\left(\frac{d\psi}{dx}\right)^2\right.\\ &\left.+[v^2p(x)-\xi(r(x)-p(x))]\psi^2(x)\right\}dx\\ &+b_{12}p(c)\psi^2(c)+b_{22}p(c+d)\psi^2(c+d)\end{aligned}$$

where ψ is completely unrestricted at $x=c$ and $x=c+d$. Obviously, the continuity conditions (15b) and (15c) are now regarded as the natural boundary conditions of the variational problem (16).

The new variational equation (16) is solved numerically, using the finite element method with the quadratic trial

TABLE II
DEFINITIONS OF SYMBOLS IN (15) AND (16)

Symbol	LSE mode	LSM mode
$\psi(x)$	$\psi_h(x)$	$\psi_e(x)$
b_{11}	-1	-1
b_{21}	1	1
b_{12}	$v \coth (vc)$	$v \tanh (vc) / p(c)$
b_{22}	$v \coth\{v[a-(c+d)]\}$	$v \tanh\{v[a-(c+d)]\} / p(c+d)$

function (11). For this purpose we divide the interval $[c, c+d]$, instead of $[0, a]$, into subintervals (or elements). Then the continuous system (16) can again be cast into the discrete form as in (12), which is the ultimate matrix eigenvalue problem to be solved numerically.

III. RESULTS

In this study, the propagation characteristics for various dielectric-slab-loaded waveguides (symmetrically or asymmetrically loaded) are investigated with emphasis on the slab of parabolic profile

$$\epsilon_r(x)=\frac{4(\epsilon_{rm}-1)}{d^2}(x-c)(c+d-x)+1, \quad c\leqslant x\leqslant c+d \tag{17}$$

and that of constant profile

$$\epsilon_r(x)=\epsilon_{rm}, \qquad c\leqslant x\leqslant c+d. \tag{18}$$

Here c, d are parameters defined in Fig. 1 and ϵ_{rm} is the maximum permittivity in the slab. Of course, the profile (18) is chosen only for the purpose of comparison or accuracy check.

For discussing the approaches which correspond to different formulations and trial functions, three numerical methods (the conventional Ritz method based on (7) and (8), the conventional finite element method on (7) and (11), and the new finite element method on (16) and (11)) are used to solve the problem (18) with exact solutions.

Typical numerical results to reflect the errors

$$\text{Error}=100\frac{k_a(\beta)-k_e(\beta)}{k_e(\beta)} \text{ percent} \tag{19}$$

in the $ka-\beta a$ diagrams for the dominant (LSE_{10}) mode are depicted in Fig. 2 for comparison. These curves are based on the three methods for the same matrix size (rank $N=5$). Here $k_e(\beta)$ is the exact wavenumber, corresponding to a given β, computed from the field-matching technique and $k_a(\beta)$ is the approximate one, corresponding to the same β, computed from one of the three numerical methods. Note that the maximum errors, associated with the new finite element method, for symmetrically and asymmetrically loaded cases are so small (of the order 10^{-2} percent) that they are represented practically by a horizontal line in Fig. 2.

By examining the results in Fig. 2 as well as the others (not shown) for the three methods one may have the

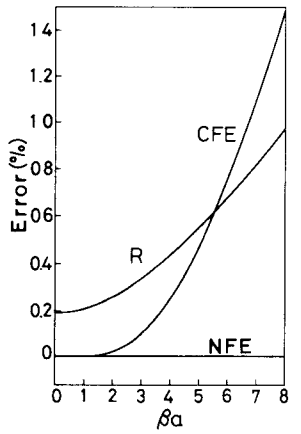

(a)

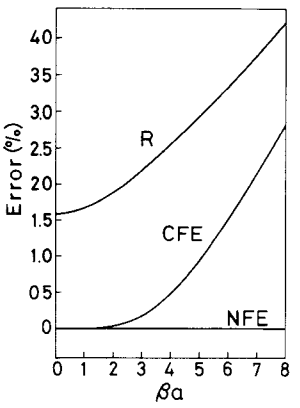

(b)

Fig. 2. Errors in $ka-\beta a$ diagrams for dominant mode by three numerical methods. Ritz method (R), conventional finite element method (CFE), and new finite element method (NFE) of same matrix size (matrix rank $N=5$) are used to solve waveguide problem with homogeneous slab loading (18) ($a/b=2, d/a=0.1, \epsilon_{rm}=100$). (a) Symmetrically loaded case ($c/a=0.45$). (b) Asymmetrically loaded case ($c/a=0.1$).

conclusions as follows. The new finite element method is superior to the conventional Ritz and finite element methods in the sense of accuracy and rate of convergence, no matter whether the waveguide is symmetrically or asymmetrically loaded. The Ritz method is efficient in solving the symmetrically loaded problem, though it is awkward in handling the LSM modes in an asymmetrically loaded one due to the difficulty in fitting the natural transition condition (5b). The conventional finite element method can satisfactorily be applied to the symmetrical- and asymmet-

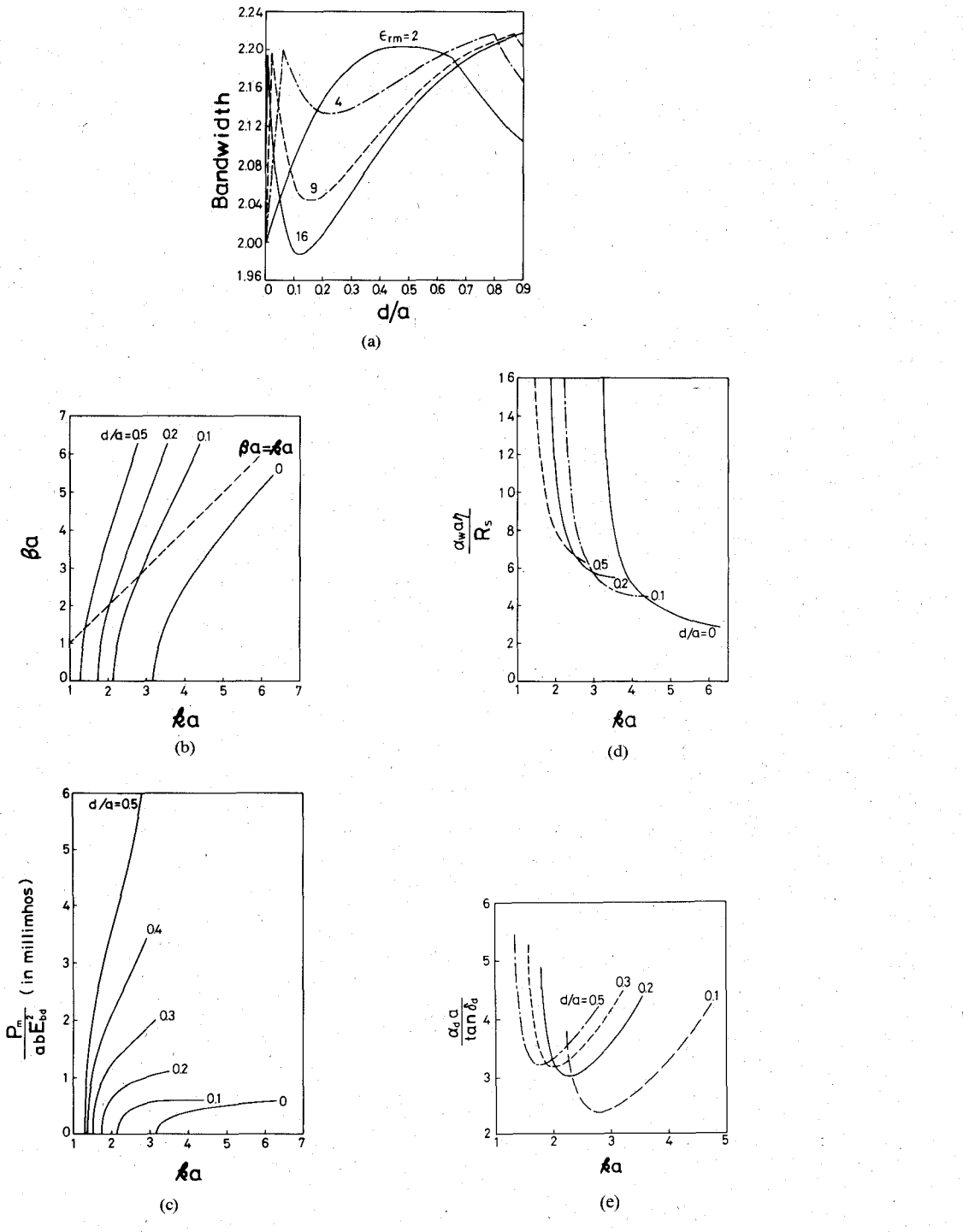

Fig. 3. Propagation characteristics for waveguide centrally loaded with slab of parabolic profile (17) ($a/b=2$). (a) Useful bandwidth. (b) Dispersion relation for dominant mode ($\epsilon_{rm}=9$). (c) Power handling capacity for dominant mode ($\epsilon_{rm}=9$). (d) Normalized wall attenuation constant for dominant mode ($\epsilon_{rm}=9, \eta=\sqrt{\mu_0/\epsilon_0}$). (e) Normalized dielectric attenuation constant for dominant mode ($\epsilon_{rm}=9$).

rical-loading cases, hence it becomes of importance whenever the Ritz method is less efficient. The new finite element method has advantages in several aspects, such as in reducing the required computer storage and in minimizing the effort in node arrangement. However, it is somewhat less flexible in mathematical formulations and actual computations.

In the following (Fig. 3(a)–(e)), various propagation characteristics of the guide centrally loaded with a slab of parabolic profile (17) are plotted and examined in detail.

The useful bandwidth is defined as the ratio of the cutoff frequency of the first higher order mode to that of the dominant mode [7], [14]. For the guide with $a>b$, the dominant mode is the LSE_{10} one, and the first higher order

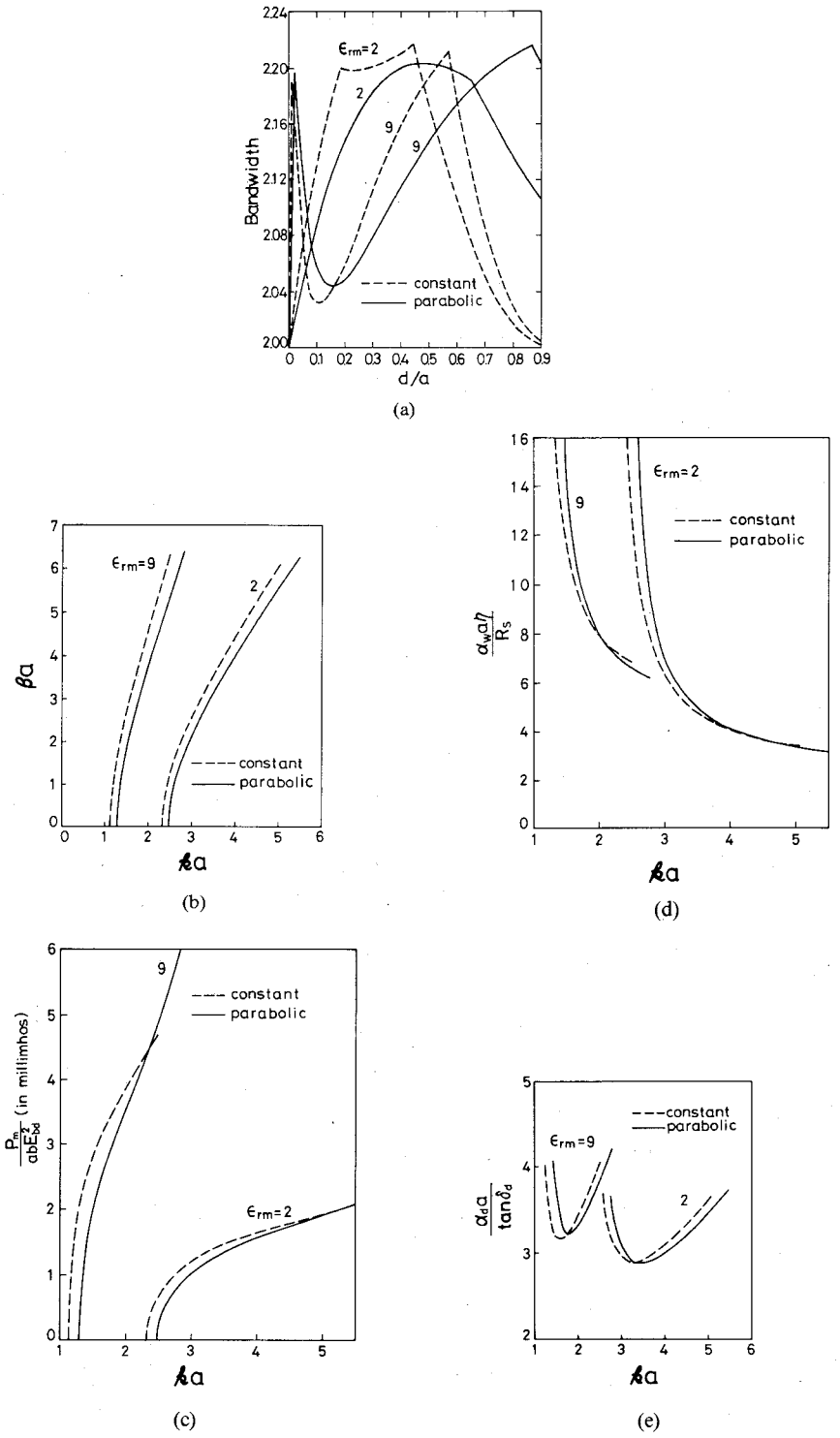

Fig. 4. Comparisons of characteristics for centrally loaded guides with parabolic and constant permittivity profiles (17) and (18) ($a/b=2$). (a) Useful bandwidth. (b) Dispersion relation for dominant mode ($d/a=0.5$). (c) Power handling capacity for dominant mode ($d/a=0.5$). (d) Normalized wall attenuation constant for dominant mode ($d/a=0.5$). (e) Normalized dielectric attenuation constant for dominant mode ($d/a=0.5$).

mode is the one among LSE_{20}, LSE_{11}, and LSM_{11} modes for which the cutoff frequency is lowest.

The power handling capacity is defined as

$$\text{PHC}=P_m/\left(abE_{bd}^2\right) \tag{20}$$

where E_{bd} is the breakdown field strength and P_m is the associated (or maximum) average power transmitted across the guide. It is assumed that the breakdown of a guide will take place at the position where the field is highest in the air regions, i.e., at the air–dielectric interface [1].

The wall and dielectric attenuation constants, α_w and α_d, for smaller conductor and dielectric losses are calculated

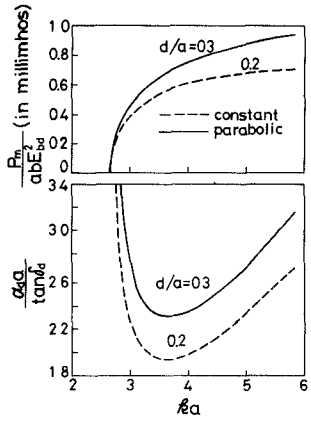

(a)

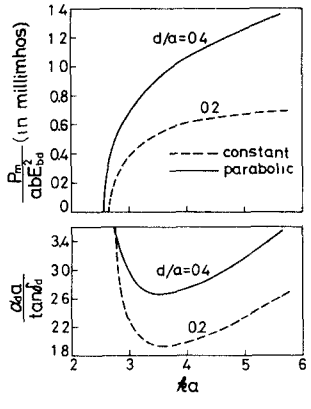

(b)

Fig. 5. Comparisons of waveguides centrally loaded with parabolic and constant profiles (17) and (18) of same permittivity height ($\epsilon_{rm}=2$, $a/b=2$). (a) Comparisons of dominant mode characteristics based on same cutoff frequency ($k_c a=2.66$). (b) Comparisons of dominant mode characteristics based on same bandwidth ($=2.20$).

from the well-known perturbation formulas [1], [2]. Plotted in Fig. 3(d) and 3(e) are the normalized attenuation constants with respect to conductor surface resistivity R_s and dielectric loss tangent $\tan\delta_d(=\epsilon_r''(x)/\epsilon_r'(x))$ which is assumed independent of x.

Depicted in Fig. 3(a) is a plot of useful bandwidth versus d/a with ϵ_{rm} as parameters. Note that for a smaller given value of ϵ_{rm} such as $\epsilon_{rm}=2$, the bandwidth is limited by the LSM_{11} (or LSE_{20}) mode depending on whether $d/a<$ (or $>$)0.65. Note also that for a given ϵ_{rm} that is not too low (for examples, $\epsilon_{rm}=4$, 9, and 16), there exist two slab widths d_1 and d_2 for which the bandwidth has two peaks. For those values of d such that $d_1 \leqslant d \leqslant d_2$, the bandwidth is limited primarily by the LSE_{11} mode. But for the values of $d \leqslant d_1$ (or $d \geqslant d_2$), the bandwidth will be determined by the LSM_{11} (or LSE_{20}) mode. Actually, the peak occurs at the particular width d_1 (or d_2) for which the cutoff frequencies for LSE_{11} and LSM_{11} modes (or those for LSE_{11} and LSE_{20} modes) are equal. Of course, an increase in the ratio a/b will lead to an increase in the useful bandwidth. However, this increase will be accompanied by a decrease in the power handling capacity. Note that the right peak is usually the maximum bandwidth available, and is nearly the same for most values of ϵ_{rm}.

In Fig. 3(b) it is of interest to note that the asymptote (the dashed line $\beta a=ka$) to the curve for $d=0$ intersects all dispersion curves at finite ka. Thus the dielectric-slab-loaded structure may support a slow wave when ka is greater than that at the intersection of solid and dashed curves.

Note that the power handling capacity for a loaded guide (Fig. 3(c)) may be less than that for an unloaded one in some frequency range if the slab is not thick enough to tolerate the high field strength in the dielectric region. Of course the power handling capacity can be increased when d or ϵ_{rm} is increased.

Note also that there may exist a certain range for ϵ_{rm}, d, and k such that the wall attenuation constant (Fig. 3(d)) can be reduced when an empty guide is dielectrically loaded.

Comparisons of the propagation characteristics for the same guiding structure ($a/b=2$) centrally loaded with slabs of parabolic and constant profiles, (17) and (18), are summarized in Figs. 4 and 5.

Fig. 4(a)–(e) first compare the results for the slabs of different profiles but of the same ϵ_{rm} and d.

In Fig. 5(a) and (b) comparisons are made, under two different bases, of the characteristics for parabolic and constant profiles with the same permittivity height ($\epsilon_{rm}=2$). The constant profile ($d/a=0.2$) and the parabolic one ($d/a=0.3$) are compared on the basis of producing the same cutoff frequency ($k_c a=2.66$), on the one hand. The same constant profile ($d/a=0.2$) and the parabolic one ($d/a=0.4$) are compared on the ground of providing the same bandwidth ($=2.20$), on the other hand.

IV. Conclusions

A numerical technique, based on the new variational formulation (16) and the finite element method, has been developed for studying the waveguide problem with an inhomogeneous dielectric slab loading. From numerical trials it is found that this new variational technique is much better than the conventional variational ones in the following aspects: accuracy, rate of convergence, and effectiveness in handling the symmetrically and asymmetrically loaded problems with permittivity discontinuities.

Various numerical results have been analyzed for the guide centrally loaded with a slab of parabolic permittivity profile. It is found that the useful bandwidth can be slightly increased by the slab loading with parabolic and constant profiles, and the propagation characteristics of both profiles are similar in general.

Acknowledgment

Discussion with Y. W. Kiang was helpful and is much appreciated.

References

[1] P. H. Vartanian, W. P. Ayres, and A. L. Helgesson, "Propagation in dielectric slab loaded rectangular waveguide," *IRE Trans. Microwave Theory Tech.*, vol. MTT-6, pp. 215–222, Apr. 1958.

[2] R. E Collin, *Field Theory of Guided Waves*. New York: McGraw-Hill, 1960.

[3] G. F. Bland and A. G. Franco, "Phase-shift characteristics of dielectric loaded waveguide," *IRE Trans. Microwave Theory Tech.*,

vol. MTT-10, pp. 492–496, Nov. 1962
[4] R. Seckelmann, "Propagation of TE modes in dielectric loaded waveguides," *IEEE Trans. Microwave Theory Tech.*, vol. MTT-14, pp. 518–527, Nov. 1966.
[5] H. R. Witt, R. E. Biss, and E. L. Price, "Propagation constants of a waveguide containing parallel sheets of finite conductivity," *IEEE Trans. Microwave Theory Tech.*, vol. MTT-15, pp. 232–239, Apr. 1967.
[6] N Eberhardt, "Propagation in the off center E-plane dielectrically loaded waveguide," *IEEE Trans. Microwave Theory Tech.*, vol. MTT-15, pp. 282–289, May 1967.
[7] F. E. Gardiol, "Higher-order modes in dielectrically loaded rectangular waveguides," *IEEE Trans. Microwave Theory Tech.*, vol. MTT-16, pp. 919–924, Nov. 1968.
[8] A. Vander Vorst and R. Govaerts, "On the accuracy obtained when using variational techniques for asymmetrically loaded waveguides," *IEEE Trans. Microwave Theory Tech.*, vol. MTT-17, pp. 51–52, Jan. 1969.
[9] G. Gonzalez and D. C. Stinson, "Propagation in rectangular waveguide partially filled with an inhomogeneous dielectric," *IEEE Trans. Microwave Theory Tech.*, vol. MTT-17, pp. 284–286, May 1969.
[10] G. Gonzalez and V. R. Johnson, "Propagation in a rectangular waveguide partially filled with a linearly varying dielectric," *IEEE Trans. Microwave Theory Tech.*, vol. MTT-18, pp. 404–406, July 1970.
[11] Z. J. Csendes and P. Silvester, "Numerical solution of dielectric loaded waveguides: I-Finite-element analysis," *IEEE Trans. Microwave Theory Tech.*, vol. MTT-18, pp. 1124–1131, Dec. 1970.
[12] T. K. Findakly and H. M. Haskal, "On the design of dielectric loaded waveguides," *IEEE Trans. Microwave Theory Tech.*, vol. MTT-24, pp. 39–43, Jan. 1976.
[13] F. E. Gardiol, "Comment on "On the design of dielectric loaded waveguides"," *IEEE Trans. Microwave Theory Tech.*, vol. MTT-25, pp. 624–625, July 1977.
[14] S. Halevy, S. Raz, and H. Cory, "Bandwidth optimization by dielectric loading," *IEEE Trans. Microwave Theory Tech.*, vol. MTT-26, pp. 406–412, June 1978.
[15] W. G. Lin, "Electromagnetic wave propagating in uniform waveguides containing inhomogeneous dielectric," *IEEE Trans. Microwave Theory Tech.*, vol. MTT-28, pp. 339–348, Apr. 1980.
[16] K. J. Bathe and E. L. Wilson, *Numerical Methods in Finite Element Analysis*. Englewood Cliffs, NJ: Prentice-Hall, 1976.
[17] C H. Chen and Y. W. Kiang, "A variational theory for wave propagation in a one-dimensional inhomogeneous medium," *IEEE Trans. Antennas Propagat.* vol., AP-28, pp. 762–769, Nov. 1980.

On the Quasi-TEM Modes in Inhomogeneous Multiconductor Transmission Lines

ISMO V. LINDELL, MEMBER, IEEE

Abstract— **We consider the general inhomogeneous shielded *N*-conductor transmission line and derive several properties for the quasi-TEM modes. The concept of quasi-TEM is deduced through an asymptotic series expansion of the fields and conditions for the propagation constant as well as the construction of the field are presented. It is seen that the problem is reduced to two static two-dimensional boundary value problems. The concepts of propagating modes and impedance modes are introduced and it is shown, that in the general case, these are not the same. The special cases of propagating impedance modes are finally discussed and are seen to exist under certain symmetry conditions of the multiconductor line.**

I. Introduction

THE INHOMOGENEOUS, uniform, multiconductor transmission line is a popular component in many microwave applications, especially in filter-directional coupler design. It is also well known that the dominant waves at the low-frequency end of the spectrum are not of pure TEM but quasi-TEM character. For a one-conductor shielded line this has been confirmed through asymptotic field analysis in [1], [2], but a solid systematic theory for multiconductor lines seems to be lacking. In what follows, the Sections II–V give the analysis and the method of constructing the quasi-TEM fields for a general inhomogeneous *N*-conductor shielded line. The construction is based on solutions of two sets of static field problems plus an eigenvalue problem for boundary conditions of the propagating modes.

The boundary condition or circuit theoretical point of view is then treated in Sections VI–IX. Previous considerations [5], [6], based on the assumed quasi-TEM character of the fields, have concentrated only on propagating modes. Being simpler at the terminations of the line, another set of modes, impedance modes, are introduced here and their relation to the propagating modes is studied. The impedance modes are defined as such voltage and current distributions on the line that are the same except for a scalar

Manuscript received October 14, 1980; revised February 27, 1981.
The author is with Helsinki University of Technology, Radio Laboratory, Otakaari 5A, 02150 Espoo 15, Finland.

0018-9480/81/0800-0812$00.75 ©1981 IEEE